ENVIRONMENTAL RESEARCH
CLIMATE

PURPOSE-LED PUBLISHING™

PAPER • OPEN ACCESS

Impacts of fire prevention strategies in a changing climate: an assessment for Portugal

To cite this article: Carlos C DaCamara *et al* 2024 *Environ. Res.: Climate* **3** 045002

ENVIRONMENTAL RESEARCH
CLIMATE

PAPER

Impacts of fire prevention strategies in a changing climate: an assessment for Portugal

Carlos C DaCamara[1], Virgílio A Bento[1,*], Sílvia A Nunes[1], Gil Lemos[1], Pedro M M Soares[1] and Ricardo M Trigo[1,2]

[1] Universidade de Lisboa, Faculdade de Ciências, Instituto Dom Luiz, Lisboa, Portugal
[2] Departamento de Meteorologia, Universidade Federal do Rio de Janeiro, Rio de Janeiro 21941-919, Brazil
[*] Author to whom any correspondence should be addressed.

E-mail: vabento@ciencias.ulisboa.pt

Keywords: climate change, wildfire risk, adaptation measures, continental Portugal, fire radiative power

OPEN ACCESS

RECEIVED
24 October 2023

REVISED
28 May 2024

ACCEPTED FOR PUBLICATION
12 June 2024

PUBLISHED
1 August 2024

Abstract

Climate change poses a formidable strain on societies worldwide, demanding viable and timely adaptation measures to ensure future prosperity while avoiding the impact of more frequent and intense extreme events, like wildfires, that affect all continents and biomes, leaving authorities grappling to respond effectively. Here, we focus on mainland Portugal that is inserted in the Mediterranean climate change hotspot and investigate the impact of different adaptation strategies on wildfire risk. Relying on an ensemble of regional climate models from the EURO-CORDEX initiative, we project fire weather index and fire radiative power for various representative concentration pathways (RCPs). Our findings reveal that very energetic fires, with energy release exceeding 1000 MW, may increase up to more than three-fold, depending on the RCP. Even under strong mitigation scenarios, the likelihood of having megafires increases by 1.5-fold. This underscores the need for proactive adaptation regardless of mitigation efforts. We present three different ignition avoidance strategies under different climate change scenarios. For all cases results indicate that a reduction between 20 and 60% is achievable for intense wildfires (above 1000 MW).

1. Introduction

Climate change imposes an overwhelming strain on individuals, companies, institutions, and governments, calling all those with responsibility to prepare viable and timely adaptation measures to secure the future prosperity of society (IPCC 2023a). This challenge affects several sectors, from agriculture (Bento *et al* 2021, Shahzad *et al* 2021) and forests (Austin *et al* 2020, Bento *et al* 2023) to health (World Health Organization 2021, Romanello *et al* 2022) and water resources (Marin *et al* 2020, van der Laan *et al* 2023). Among other natural hazards, weather-driven extreme events like vegetation fires, droughts, heatwaves, and extreme precipitation, including flash floods, are expected to take a toll on society as we know it (IPCC 2023b).

Wildfire regimes are projected to change considerably worldwide due to climate change (Krawchuk *et al* 2009, Pausas and Keeley 2021). Recent studies provide plenty of evidence that support to a large extent this shift, namely in what concerns some of the most destructive and intense fires that have occurred in recent years in Australia, California, and the Amazon Forest (Keeley and Syphard 2019, Boer *et al* 2020, Libonati *et al* 2021, 2022). Located in a climate change hotspot (Giorgi 2006, Diffenbaugh and Giorgi 2012, Sánchez-Benítez *et al* 2018) at the western tip of the Mediterranean, the Iberian Peninsula, and Portugal in particular, is well-known for its summer fire occurrences, extensively studied by the scientific community (Trigo *et al* 2006, 2016, Garcia-Herrera *et al* 2010, Amraoui *et al* 2013, DaCamara *et al* 2014, Russo *et al* 2017, Nunes *et al* 2019, Turco *et al* 2019, Calheiros *et al* 2021, Bento *et al* 2022, Ramos *et al* 2023, Santos *et al* 2023).

From 1980 to 2023 wildfires in mainland Portugal burned a total of 4 987 678 hectares (San-Miguel-Ayanz *et al* 2023), an area equivalent to 54% of the territory. In 2017, the total amount of burned area exceeded 500 000 ha and resulted in over 100 human fatalities (Ramos *et al* 2023). The single fire event that took place in August 2018 in Algarve (southern Portugal) was responsible for more than 25 000 ha

of total burned area, destroyed dozens of homes and claimed thousands of animal lives (DGAPPF/DDFVAP 2018). The recent 2022 fire season witnessed record-breaking fire danger indices across the country that steered a large fire event that burned a considerable portion of the Serra da Estrela mountain range, a UNESCO Geopark and Portugal's largest natural park (Mendonça and Máguas 2023). All these fire events caused substantial social and economic losses, with the 2017 fire season alone costing more than 1000 000 000 € (Ramos *et al* 2023), the event of 2018 in Algarve leaving over 100 people homeless (DGAPPF/DDFVAP 2018), and the event of 2022 in Serra da Estrela affecting severely tourism and local producers (Mendonça and Máguas 2023). Both the amount of burned area and the severity of fire events make Portugal the country most affected by wildfires among Mediterranean countries.

As in most inhabited regions of the world, wildfire activity in Portugal results from complex linkages among climate, landscape, and human activity. A recent striking example of this interplay is the megafire event that took place on 15 October 2017, that accounted for the all-time record of about 220 000 ha of burned area in 24 h, an amount that is twice the annual mean in 1980–2023. The event was the outcome of vegetation stress because of a prolonged drought, combined with extreme meteorological conditions associated with the passage of hurricane Ophelia off-coast of Portugal and with a record number of negligent ignitions set up by farmers in a critical day of meteorological fire danger (Ramos *et al* 2023).

Fire activity is therefore modulated by natural and anthropogenic factors. The former include topography, vegetation and weather conditions, with the rainy and mild winters followed by warm and dry summers favoring the occurrence of wildfire events, especially in the mountainous regions of Central and Southern Portugal (Pereira *et al* 2005). Ignitions are anthropogenic for the most part, and reasons are as varied as preparing fields for pastures or agriculture, negligence, and arson; landcover and land use are vastly related to socio-economic activities; and climate is mostly forced by human activities and emissions. Depopulation of rural areas and associated conversion of agricultural fields into forest plantations, shrublands or woodlands are also major anthropogenic factors that contribute to increased fuel (Pausas *et al* 2008).

Recent records point towards a 'new normal' where frequent extreme fire danger conditions and associated large fire events become part of everyday life during the warmer summer months (Bento *et al* 2022). This prospect becomes even more worrisome when considering the non-stationary nature of climate evolution under climate change forcing and therefore the inevitability that this 'new normal' is bound to be exceeded, according to climate change projections until the end of the 21st century. A recent study (Bento *et al* 2023) points out that summer fire danger in the Iberian Peninsula is expected to substantially increase in the future, with an expansion of the fire season from June to September. Northwestern Iberia, including northern Portugal and northwestern-to-central Spain, is projected to experience the largest increases in fire danger. These regions are particularly vulnerable due to their fire-prone vegetation (Trigo *et al* 2006). However, projections differ among different scenarios, emphasizing the need for distinct adaptation strategies to be promptly adopted by stakeholders and authorities.

The door to climate change adaptation is now open, urging companies, institutions, and governments to make efforts in developing and adopting new strategies (IPCC 2023a). This framework has steered a new large scale research project for Portugal, namely the National Roadmap for Adaptation XXI—Portuguese Territorial Climate Change Vulnerability Assessment for the XXI Century (RNA2100) (Soares and Lima 2022, Cardoso *et al* 2023, Lima *et al* 2023a, 2023b, Soares *et al* 2023a, 2023b). Its main objectives include the development of state-of-the-art regional climate projections and definition of adaptation strategies for Portugal, with particular emphasis on wildfires in the context of a changing climate.

With the aim of assessing climate change impacts and implications, experiments focusing on dynamic or statistical downscaling of global climate models (GCMs) were designed within the framework of projects such as the coordinated regional downscaling experiment (CORDEX) (Giorgi *et al* 2009, Jacob *et al* 2020). Many authors have taken advantage of ensembles composed by several continental-scale simulations from CORDEX to assess climate change projections on various key variables in order to evaluate wildfire danger from a European scale to that of the Iberian Peninsula and Portugal. These studies systematically point to a decrease in mean precipitation along with an increase in extreme precipitation events (Soares *et al* 2017), an increase in maximum and minimum temperature independently of the season of the year and emission scenario (Cardoso *et al* 2019), and a decrease in 10-m wind speed over the northernmost part of Portugal in autumn and winter and an increase during summer months over the central country (Nogueira *et al* 2019). Moreover, a number of works have recently focused on CORDEX multi-model experiences to analyze projections of wildfire danger indices in regions scattered over the globe (Faggian 2018, Ruffault *et al* 2018, Varela *et al* 2019, Trnka *et al* 2021).

The Canadian forest fire weather index system (CFFWIS) is one of the most well-known and widely used set of meteorological fire danger indices. CFFWIS is composed of six components that rate fuel moisture and weather conditions' effects on fire behavior (Van Wagner 1974). The components rely on empirical and

semi-empirical relations between meteorological variables (temperature, precipitation, relative humidity, and wind speed) and fuel moisture, characterizing the level of dryness of a standard fuel, namely that of a generalized Canadian jack pine forest (Stocks *et al* 1989). These components include the fine fuel moisture code (FFMC), the duff moisture code (DMC), the drought code (DC), the initial spread index (ISI), the build-up index (BUI), and the fire weather index (FWI). FWI provides valuable information on the role of meteorological conditions in favoring the build-up and spread of wildfires, and is particularly suitable for assessing meteorological fire danger over Mediterranean Europe; for instance, information about FWI is now an operational part of the emergency management services within the EU Copernicus program—the Fire Danger Forecast module of the European forest fire information system (EFFIS) (San-Miguel-Ayanz *et al* 2012). FWI has also been successfully used to improve the quality of fit of statistical models of the distribution of hotspots related to vegetation fires, either in terms of duration (DaCamara *et al* 2014) or energy released (Pinto *et al* 2018); these models are on the basis of the fire risk map product that is operationally disseminated by the satellite application facility for land surface analysis (LSA SAF) that is part of the ground segment of EUMETSAT (Trigo *et al* 2011).

In a recent study, DaCamara *et al* (2023) showed that the logarithm of fire radiative power (FRP), i.e. the rate of energy released by vegetation fires, follows a distribution consisting of a doubly truncated lognormal central body with generalized Pareto (GP) lower and upper tails. Nunes *et al* (2023) then showed that the model is improved by incorporating FWI as a covariate in the parameters of the model, and that the improved model could be used to generate synthetic values of FRP associated to prescribed values of FWI.

The present study aims at extending this approach to characterize fire activity in Portugal for different projected scenarios throughout the 21st century and, based on FWI projections, to assess the impact of ignition avoidance strategies. We propose in this work to address the two following questions: (1) What is the projected change in the probability of intense fires in continental Portugal, and how is this change affected by different greenhouse gas emission scenarios? (2) What is the impact of different ignition avoidance strategies? Should they be implemented over pre-defined periods, and encompassing the territory as a whole? Or should they be confined to specific regions and specific days according to the level of fire danger? Answers to these questions will be provided by leveraging an ensemble of regional climate models (RCMs) from the EURO-CORDEX initiative, MODIS observations of FRP, and the design of simple but illustrative strategies for fire reduction.

2. Datasets

The observations of remotely sensed FRP, as well as reanalysis and modeled meteorological data used to compute FWI, are described in the following subsections.

2.1. Observations of radiative power released by fires

FRP was obtained based on the moderate resolution imaging spectroradiometer (MODIS) instrument aboard the Terra and Aqua satellites, namely from MODIS Collection 6 Active Fire Product (Giglio *et al* 2020). The data consists of 63 942 hotspots, i.e. pixels characterized by thermal anomalies associated to vegetation fire activity that were recorded over continental Portugal by the MODIS instrument. Data spans the 20 year period from 2001 to 2020 and, for each hotspot, information consists of geographical location, calendar date, occurrence time, and FRP estimates. Figure 1 shows a map of the vegetation cover over Portugal (left) and another one with the location of each hotspot of the entire dataset (right). Land cover data are from the Copernicus Global Land Service (Version 3), covering the period 2015–2019 (Buchhorn *et al* 2020). The original 23 vegetation cover classes were stratified into six primary categories: shrubland, cropland, closed forest, open forest, built-up, and sparse vegetation. Hotspots concentrate over the forests and shrublands of northern, central, and SW Portugal, as well as over the croplands in the NW.

2.2. Meteorological data from ERA5

The meteorological variables required to estimate the reference FWI were retrieved from the European Centre for Medium Range Weather Forecasts (ECMWF) ERA5 reanalysis (Hersbach *et al* 2020). Information consists of hourly values of 2 m temperature, 2 m dew point temperature, zonal and meridional components of wind speed at 10 m, and accumulated precipitation. Data is available at a spatial resolution of $0.25° \times 0.25°$ and spans the period from 2001 to 2020 (in agreement with the period of observations of FRP).

ERA5 has been extensively used to compute FWI in several regions of the world (Vitolo *et al* 2020, Carrillo *et al* 2022, Santos *et al* 2023). For instance, the EFFIS of the Copernicus emergency management service makes available a global dataset of fire danger indices based on the CFFWIS using as input reanalyzed meteorological variables from ERA5 (Vitolo *et al* 2020).

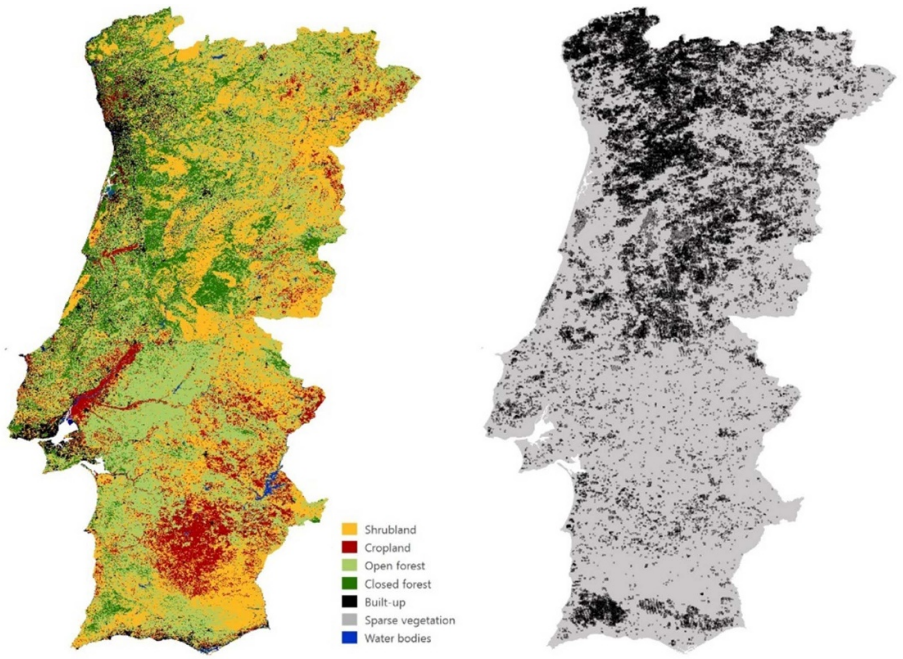

Figure 1. Geographical distribution over Portugal of classes of vegetation cover (left) and of vegetation fire hotspots (right) recorded by MODIS from 2001 to 2020.

Table 1. EURO-CORDEX RCMs used in this study, along with the responsible entities and the forcing GCMs. The 13 simulations have historical, RCP2.6, RCP4.5, and RCP8.5 scenarios.

RCM	Institute	GCM
CCLM4-8-17	CLM	EC-Earth
ALADIN63	CNRM	CNRM-CM5
HIRHAM5	DMI	EC-Earth
		HadGem2-ES
REMO2015	GERICS	NorESM1-M
RACMO22E	KNMI	CNRM-CM5
		EC-Earth
		HadGem2-ES
REMO2009	MPI	MPI-ESM-LR
RCA4	SMHI	EC-Earth
		HadGem2-ES
		MPI-ESM-LR
		NorESM1-M

2.3. EURO-CORDEX model data

The EURO-CORDEX high-resolution simulations, performed under the CORDEX effort (Jacob *et al* 2014, 2020), provide a large number of regional climate runs over a common domain. For this study, we relied on RCM model runs corresponding to the dynamical downscaling of the original CMIP5 GCM ensemble, with a horizontal resolution of 0.11°. Each ensemble comprehends a historical period (1971–1990), and three projected ones along the 21st century (namely, the begin-century 2011–2030, the mid-century 2041–2060, and the end-century 2071–2090) considering emission scenarios RCP2.6, RCP4.5, and RCP8.5. From the full set of EURO-CORDEX RCM simulations available in the Earth system grid federation (ESFG) data portal, only 13 of them include runs for both historical and the three considered future scenarios. Hence, these 13 simulations were selected to be used in our study (table 1).

EURO-CORDEX simulations have undergone extensive evaluation for the current climate. The outcomes demonstrate notable improvements in capturing the intrinsic temporal and spatial variations characteristic of the European climate (Vautard *et al* 2013, Kotlarski *et al* 2014, Katragkou *et al* 2015, Prein *et al* 2016). In an assessment by Herrera *et al* (2020), EURO-CORDEX RCMs showed good skills in reproducing precipitation and temperature patterns across the Iberian Peninsula. The findings highlighted strong spatial consistency between observations and simulations. Comparable evaluations were conducted in Portugal by Soares *et al* (2017) and Cardoso *et al* (2019). These studies also underscored substantial

agreement between the multi-model EURO-CORDEX ensemble and observations, showcasing marked improvements compared to preceding regional climate initiatives like PRUDENCE and ENSEMBLES (Soares *et al* 2012). The benefit of employing high-resolution EURO-CORDEX simulations was quantified for precipitation (Soares and Cardoso 2018, Careto *et al* 2022a), temperature (Cardoso and Soares 2022; Careto *et al* 2022b), and wind (Molina *et al* 2023). The analyses unveiled added value of using these high-resolution data in depicting the variable patterns of temperature and precipitation across Europe, particularly over the Iberian region and for extreme events the analyses unveiled significant added value in depicting these variable patterns across Europe, particularly for the Iberian region and especially for extreme events. EURO-CORDEX RCMs also exhibited skill in representing near-surface wind speeds both onshore (Vautard *et al* 2013, Moemken *et al* 2018, Nogueira *et al* 2019) and offshore (Soares *et al* 2017).

3. Methods

In this section, a comprehensive overview of the methods employed is provided. To potentiate the use of the 13 EURO-CORDEX models, we adopted a weighted multi-model ensemble approach specifically calibrated for Portugal. The model weights are calculated based on each model's ability to accurately represent the multi-variable climate of Portugal. As described in detail in Lima *et al* (2023a), this multi-model approach can be applied to the computation of FWI (Bento *et al* 2023) and future climate indices (Lima *et al* 2023b), heatwaves (Cardoso *et al* 2023), and drought and soil moisture assessment (Soares and Lima 2022, Soares *et al* 2023a). By using this refined multi-variable method to create the ensemble, we mitigate the uncertainty inherent in climate modeling, that allows obtaining more accurate regional climate projections (Brunner *et al* 2019, Eyring *et al* 2019). Throughout this study, the results are consistently presented in the form of the multi-model ensemble.

3.1. Computing the FWI

All CFFWIS components, namely DC, DMC, FFMC, ISI, BUI, and FWI were estimated following Van Wagner (1987). As in Moriondo *et al* (2006), Carvalho *et al* (2009), Giannakopoulos *et al* (2009), and Bento *et al* (2023), the CFFWIS components were computed based on daily mean 2 m temperature, relative humidity, and 10 m wind speed, and on daily accumulated precipitation, and are estimated daily for each grid-point of the reference period (based on ERA5 reanalysis) and, for each individual model, for the historical and future periods (the latter over the three different emission pathways).

It is worth noting that the use of daily mean data instead of data at 12-noon introduces systematic biases when computing CFFWIS components (Herrera *et al* 2013), a problematic issue when assessing the impact of climate change on meteorological fire danger. In our study, this issue is circumvented because FWI is not used directly but as a covariate in statistical models of FRP. As discussed in the next section, the statistical models are fitted to FRP using FWI as derived from daily mean data, and the impact of climate change is then assessed using again values of FWI based on daily mean data from the different climate scenarios.

Then, for each of the 63 942 MODIS hotspots spanning 2001–2020, we assigned the value of FWI of the day of observation at the nearest ERA5 grid-point. Since the historical period from the EURO-CORDEX RCMs encompasses the period between 1971–2005 and runs are not synchronized in time, the last 20 years were extracted and assigned to the MODIS hotspots from 2001 to 2020. The same procedure is used for the three future periods, namely the beginning of the century 2011–2030, the middle of the century 2041–2060, and the end of the century 2071–2090, for representative concentration pathways (RCPs) 2.6, 4.5, and 8.5, and for the 13 RCMs. For all periods the location of the hotspots is kept unchanged.

RCMs are affected by systematic errors (biases) when compared to observations or reanalyzes, which arise from limitations such as the horizontal and vertical resolutions and physical or numerical parameterizations within the models (Rummukainen 2010, Soares *et al* 2012, Rocheta *et al* 2017, Herrera *et al* 2020). As biases in RCMs have been thoroughly characterized, different approaches have been put forward for their correction (Maraun *et al* 2017, 2019, Gutiérrez *et al* 2019, Hertig *et al* 2019, Soares *et al* 2019). Accordingly, bias correction techniques have become a standard procedure in climate change studies, attempting to correct systematic errors in climate simulations and increase their agreement with reference datasets.

Here, both the historical and future projected FWIs were corrected using the Empirical Gumbel Quantile Mapping (EGQM), a bias correction technique developed and tested by Lemos *et al* (2020b), Lemos *et al* (2020a)). The EGQM technique consists of correcting a simulated empirical cumulative distribution function (ECDF; Wilks 2011) by adding a correction term to each (pre-selected) quantile. The quantiles are defined by a standard Gumbel distribution (SGD; Gumbel 1935), focusing on the upper tail of the distribution (a paramount characteristic when studying extreme events such as wildfires).

In order to correct the historical FWIs, a set of $n_q = 20$ quantiles is selected, following an SGD, beginning with the 1st and ending with the 99.9th quantiles. The correction term is the difference between the inverse

ECDFs of the reference ($\mathrm{ECDF}^{\mathrm{REF}^{-1}}$) and the simulated ($\mathrm{ECDF}^{\mathrm{SIM}^{-1}}$) data. This difference is calculated and applied for each pre-selected quantile, as follows:

$$X(q_i) = \mathrm{ECDF}^{\mathrm{REF}^{-1}}(q_i) - \mathrm{ECDF}^{\mathrm{SIM}^{-1}}(q_i), i = 1, \ldots, n_q, \quad (1)$$

$$\mathrm{SIM}^{\mathrm{C}}(q_i) = \mathrm{SIM}(q_i) + X(q_i), \; i = 1, \ldots, n_q, \quad (2)$$

where SIM corresponds to the originally simulated FWIs and $\mathrm{SIM}^{\mathrm{C}}$ to the bias corrected ones. The correction terms are linearly interpolated between the pre-selected quantiles, and all data outside the defined quantile range is extrapolated considering the correction terms found for the first and last pre-selected quantiles.

One of the main assumptions in the bias correction is that the bias behavior does not change in time, i.e. systematic errors remain stationary between historical simulations and future projections (Haerter *et al* 2011). Accordingly, the future FWI projections are corrected using the same correction terms found for the historical period.

3.2. Fitting the statistical model of FRP

Following DaCamara *et al* (2023) the distribution of the decimal logarithm of FRP (hereafter log10(FRP)) associated to vegetation fire hotspots in Portugal is modeled by a doubly truncated lognormal central body with a reversed GP lower tail and a GP upper tail. The cumulative density function (CDF) of this distribution is characterized by eight parameters:

$$\begin{aligned} P(\log 10(\mathrm{FRP}) < x) &= F_0(x; \kappa_l, \sigma_l, x_l, \lambda_b, \sigma_b, \kappa_u, \sigma_u, x_u) \\ &= \begin{cases} bc\left[1 - \left(1 + \kappa_l \frac{x_l - x}{\sigma_l}\right)^{-\frac{1}{\kappa_l}}\right], & x < x_l \\ bc + \frac{b}{2C}\left[\mathrm{erf}\left(\frac{\ln x - \lambda_b}{\sqrt{2}\sigma_b}\right) - \mathrm{erf}\left(\frac{\ln x_l - \lambda_b}{\sqrt{2}\sigma_b}\right)\right], & x_l \leqslant x \leqslant x_u \\ bc + b + ba\left[1 - \left(1 + \kappa_u \frac{x - x_u}{\sigma_u}\right)^{-\frac{1}{\kappa_u}}\right], & x > x_u \end{cases} \end{aligned} \quad (3)$$

where the distribution F_0 depends on the shape (κ_l) and scale (σ_l) parameters of the reversed GP lower tail, the transition point (x_l) from the lower tail to the central body, the location (λ_b) and scale (σ_b) parameters of the truncated lognormal central body, the shape (κ_u) and scale (σ_u) parameters of the GP upper tail, and the transition point (x_u) from the central body to the upper tail, and where erf denotes the error function and a, b and c are normalizing constants. Parameters are estimated by maximizing the log-likelihood function using an independent and identically distributed (i.i.d.) sample of observed data.

Estimates of the eight parameters of the model are obtained by maximizing the log-likelihood function of the entire sample of 63 942 hotspots. Then the same procedure is applied to 100 subsamples, each one made of 10 000 randomly selected events from the entire sample. We, therefore, obtain 100 sets of maximum likelihood estimates of the eight parameters of the model. This procedure allows assessing both the effects of potential spatial and temporal dependence in the data as well as obtaining ranges of uncertainty for the estimated parameters of the model. Model performance is visually checked by means of Q–Q plots and goodness of fit is assessed using the Anderson–Darling test of whether a given sample of data is drawn from the truncated lognormal distribution with GP tails; p-values of the Anderson–Darling statistic, p_{AD}, are estimated by randomly generating 1000 data samples from the fitted distribution, and the hypothesis is rejected at the 5% level in case $p_{\mathrm{AD}} < 0.05$. Details can be found in DaCamara *et al* (2023).

The eight-parameter model is then improved by introducing FWI as a covariate of the parameters, namely by assuming:

$$\begin{aligned} \kappa_l &= -\exp(m_{\kappa_l} \times FWI + b_{\kappa_l}) \\ \sigma_l &= +\exp(m_{\sigma_l} \times FWI + b_{\sigma_l}) \\ x_l &= +\exp(m_{x_l} \times FWI + b_{x_l}) \\ \lambda_b &= m_{\lambda_b} \times FWI + b_{\lambda_b} \\ \sigma_b &= +\exp(m_{\sigma_b} \times FWI + b_{\sigma_b}) \\ \kappa_u &= -\exp(m_{\kappa_u} \times FWI + b_{\kappa_u}) \\ \sigma_u &= +\exp(m_{\sigma_u} \times FWI + b_{\sigma_u}) \\ x_u &= +\exp(m_{x_u} \times FWI + b_{x_u}) \end{aligned} \quad (4)$$

This assumption leads to the following model with 16 parameters whose estimates are again obtained by maximizing the log-likelihood function of the entire sample of 63 942 hotspots together with the associated values of FWI:

$$P(\log 10\mathrm{FRP} < x|FWI) = F_1\left(x, FWI; m_{\kappa_l}, b_{\kappa_l}, m_{\sigma_l}, b_{\sigma_l}, m_{x_l}, b_{x_l}, m_{\lambda_b}, b_{\lambda_b}, m_{\sigma_b}, b_{\sigma_b}, m_{\kappa_u}, b_{\kappa_u}, m_{\sigma_u}, b_{\sigma_u}, m_{x_u}, b_{x_u}\right). \tag{5}$$

Performance of the 16-parameter model is compared with that of the 8-parameter model using the Bayes Factor and the Vuong's closeness test. Denoting by BIC_0 and BIC_1 the Bayesian Information Criterion scores of the 8- and 16-parameter models, respectively, the Bayes Factor, B_{01}, is given by $B_{01} = \exp\left[\frac{1}{2}\left(BIC_1 - BIC_0\right)\right]$ and there is strong evidence that the 16-parameter model (the alternate model) is more performant than the 8-parameter model (the null model) when $B_{01} < 0.1$. The Vuong test is based on the closeness statistic V that depends on the sum and the variance of the individual log-likelihood ratio between the 16- and the 8-parameter models as well as on the number of parameters of the models and the size of the sample. When $V > 1.96$ the null hypothesis that performance of the eight-parameter model is better than that of the 16-parameter model is rejected at the 5% significance level. Details can be found in Nunes *et al* (2023).

Synthetic values of log10(FRP) associated to a given prescribed value of FWI may be obtained by randomly generating values uniformly distributed in the interval $[0, 1]$ and then inverting F_1 with FWI fixed to the prescribed value. An estimate of the distribution of log10(FRP) associated to a set of FWI values may therefore be obtained by applying the procedure to each value of FWI; the larger the number of generated values of log10(FRP) associated to each FWI, the closer the generated sample is to the distribution. Synthetic values of log10(FRP) were accordingly generated using the sets of FWI associated to the locations of the 63 942 pairs of log10(FRP) for the historical period and for the three future 20 year windows corresponding to RCP 2.6, RCP 4.5, and RCP 8.5 scenarios. For each value of FWI, 50 random numbers in the interval $[0, 1]$ were generated, and 50 synthetic values of log10(FRP) were then obtained by inverting the 16-parameter model.

3.3. Projecting probabilities of log10(FRP) into the 21st century

Generated synthetic values of log10(FRP) are analyzed by comparing the respective curves of probability of exceedance that are defined as 1-CDF. Comparison is performed by calculating the exceedance ratio function defined as the ratio between the curve of probability of exceedance of log10(FRP) in a given future period and that for the historical period.

3.4. A sensitivity analysis to different fire prevention strategies

Fire prevention strategies are compared by reducing the size of the synthetic samples of log10(FRP) by randomly eliminating a pre-defined fraction of values when they are associated to values of FWI within a given range. The fraction of values to be randomly eliminated and the ranges of FWI are defined according to the chosen ignition avoidance strategy. We will test the impact of three strategies on the probability of occurrence of high intensity fires, as hereby described:

- Strategy 1: this strategy involves randomly reducing 50% of values of log10(FRP) that are associated to values of FWI that are larger than the median of the sample.
- Strategy 2: under this strategy, the reduction fraction varies according to the range of FWI of the sample. When FWI falls between the 75th and 90th percentiles of the sample, 50% of the log10(FRP) instances are randomly reduced. When FWI falls between the 90th and 95th percentiles of the sample, there is a 90% reduction of log10(FRP) instances. Finally, when FWI exceeds the 95th percentile of the sample, even stricter measures are adopted leading to a 95% reduction in log10(FRP) instances.
- Strategy 3: this methodology only involves randomly reducing 95% of the log10(FRP) instances when FWI surpasses the 95th percentile of the sample.

The impact of each strategy is then quantified by the respective percentage reduction defined as:

$$\text{impact } (\%) = \frac{\mathrm{exc}\left(\mathrm{FRP}_{\text{original}}\right) - \mathrm{exc}\left(\mathrm{FRP}_{\text{filtered}}\right)}{\mathrm{exc}\left(\mathrm{FRP}_{\text{original}}\right)} \times 100 \tag{6}$$

where $\mathrm{exc}\left(\mathrm{FRP}\right)$ is the probability of exceedance of a given log10(FRP) value for the original and the filtered datasets according to the Strategy considered. This exercise is repeated for ERA5, the 13-member EURO-CORDEX historical RCM ensemble, as well as the future ones, for the three scenarios and time windows. The percentile of FWI is computed for ERA5 and for the historical period. For the future scenarios, the value used of the percentile is the one obtained from the historical for climate change assessment.

3.5. Schematic overview of the methods

A simplified schematic of the methodology is presented in figure 2.

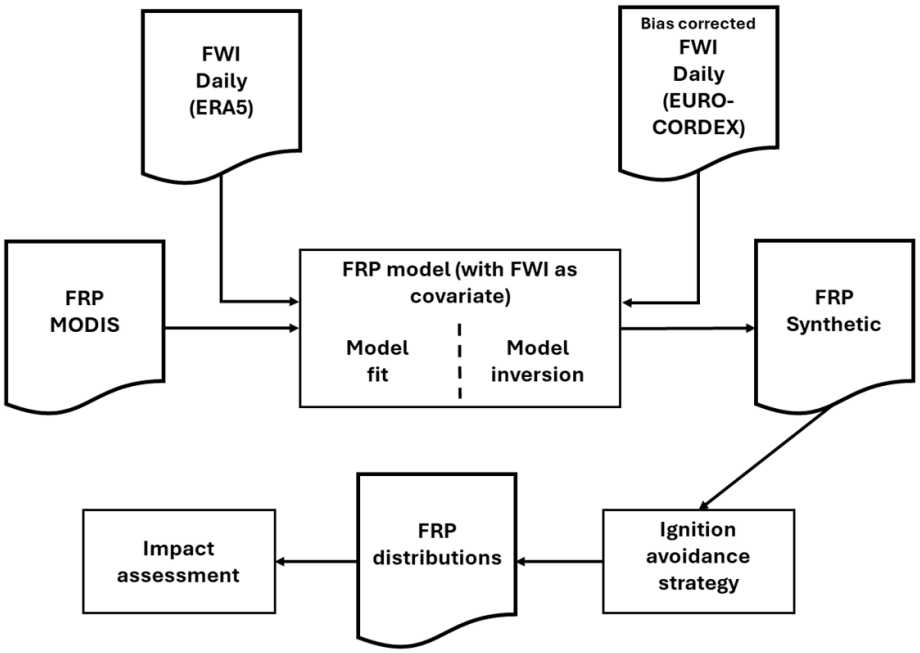

Figure 2. Flowchart of the methodology followed in this work.

4. Results

FWI from the EURO-CORDEX historical period exhibits a considerable bias when compared to ERA5. For instance (figure 3(a)), the CDF of historical FWI presents large departures from ERA5 FWI (dark red curve) for lower FWI values, with more than 70% of the cases having values below 20, whereas this amount reduces to about 55% of the cases for ERA5 FWIs (black curve). When the bias is corrected by applying the EGQM method to the historical FWI, the multi-model ensemble representation (blue curve) is substantially improved, and closely follows that for ERA5 FWIs.

The bias correction was also applied to future FWI values (figures 3(b)–(d)). It may be observed that, over the course of the century, the projected FWI curves consistently shift to the right. During the initial period (2011–2030), the projections for all three scenarios exhibit a slight shift to the right, with no clear dominant scenario. The changes of FWI were tested for their statistical significance, by means of a Kolmogorov–Smirnov test, and all the changes are statistically significant at the 95% confidence level. As we move towards the middle and end of the century, pronounced differences emerge between the scenarios. For both periods, the RCP 8.5 scenario displays a conspicuous shift to the right compared to the other RCPs, the difference becoming larger for 2071–2090. For instance, historical FWIs exceeding 20 occur in about 45% of the cases, whereas in 2041–2060 the projected exceedance rises to about 55% for RCP 2.6, 60% for RCP 4.5, and above 60% for RCP 8.5.

It is worth noting that very high values of FWI (exceeding 40) are observed in about 4% of the cases during the historical period, but in 2041–2060 (2071–2090) this fraction increases to about 8% (5%) for RCP 2.6, 9% (9%) for RCP 4.5, and 12% (15%) for RCP 8.5. This emphasizes the increased severity of fire weather conditions as we progress into the future under different climate scenarios.

The eight-parameter model of FRP was fitted to the entire dataset of 63 942 hotspots recorded over Portugal by maximizing the log-likelihood of the sample. Maximum likelihood estimates were also obtained from the 100 subsamples of 10 000 randomly selected events from the dataset. As shown in figure 4 (left panel), the plots of the CDF of the eight-parameter model with maximum likelihood estimates as obtained from the entire sample (red curve) virtually overlap over the entire support those obtained from the 100 subsamples (black curves). This is an indication of the robustness of the results, and of the negligible effect of the potential spatial and temporal dependence in the hotspots. The p-value of the Anderson–Darling test ($p_{\mathrm{AD}} = 0.18$) is larger than 0.05 indicating that the hypothesis that the sample follows a log-normal distribution with GP tails cannot be rejected at the 5% level. In turn, as shown in figure 4 (right panel), the QQ plot of empirical quantiles derived from the sample versus the theoretical quantiles obtained from the model closely follows the 1:1 line, the exception being a very small fraction of very low and very high values of log FRP that slightly deviate from it.

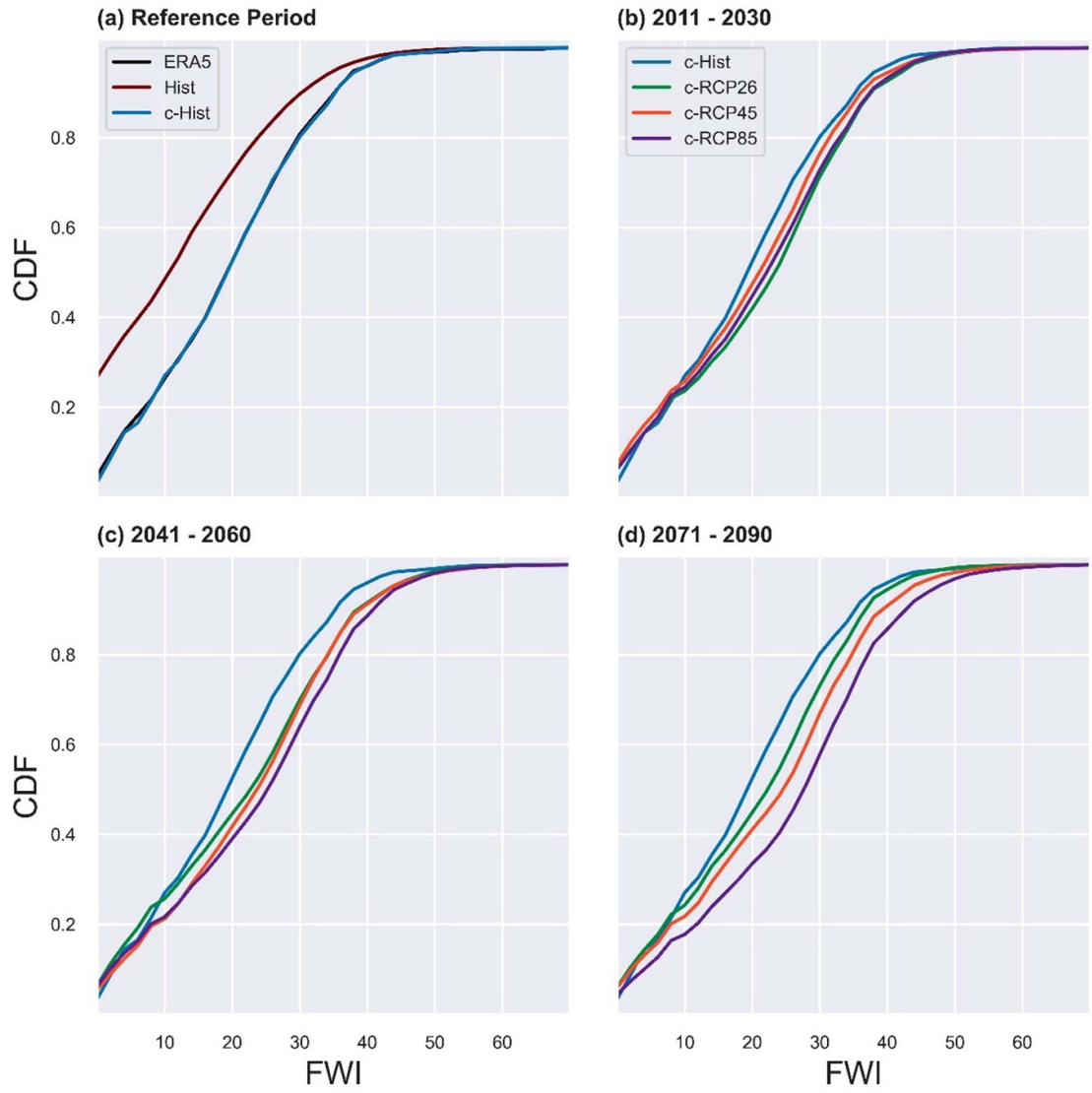

Figure 3. Distribution of FWI on vegetation fire hotspots as CDF (a) from ERA5 (solid black line), multi-model ensemble for the historical period (HIST; solid dark red line), and the bias corrected multi-model ensemble for the historical period (c-HIST; solid blue line). CDFs of bias corrected multi-model ensemble FWI for historical and projected scenarios RCP 2.6 (green line), RCP 4.5 (orange line), and RCP 8.5 (purple line) for the three 20-year future periods 2011–2030 (b), 2041–2060 (c), and 2071–2090 (d).

The 16-parameter model of log FRP with FWI as covariate, as obtained from the fitting to the 63 942 pairs of log10(FRP) and FWI that were recorded in Portugal during 2001–2020, presents, as expected, a clear sensitivity to FWI (figure 5). The CDF curves displace to the right with increasing FWI, an indication that the higher the fire meteorological danger, the larger the probability of exceedance of a given value of log10(FRP). The value obtained for the Bayes Factor, $B_{01} = 0$, provides strong evidence that the 16-parameter model is more performant than the 8-parameter model; confirming this result, the value obtained for the Vuong statistic, $V = 49$, indicates that the null hypothesis that performance of the 8-parameter model is better than that of the 16-parameter model is rejected at the 5% significance level.16-parameter model is rejected at the 5% significance level.

Figure 6(a) presents the distribution of synthetic values of log FRP as generated by the 12-parameter model using the sets of FWI derived from ERA5 (solid black line), along with those generated from the uncorrected (solid dark red line) and bias-corrected (solid blue line) historical multi-model ensemble. Results reflect the benefit of implementing the bias correction procedure as the distribution of log10(FRP) using corrected values of FWI from the historical period virtually coincides with that obtained with FWI from ERA5, whereas the curve obtained from uncorrected values presents a notable bias towards lower energies released by fires. Figures 6(b)–(d) also present the distributions of synthetic values of log10(FRP) generated using projected values of FWI for the different climate scenarios. As expected, for all subperiods considered there is a displacement of the CDF curves towards the right when going from RCP 2.6 to RCP 4.5,

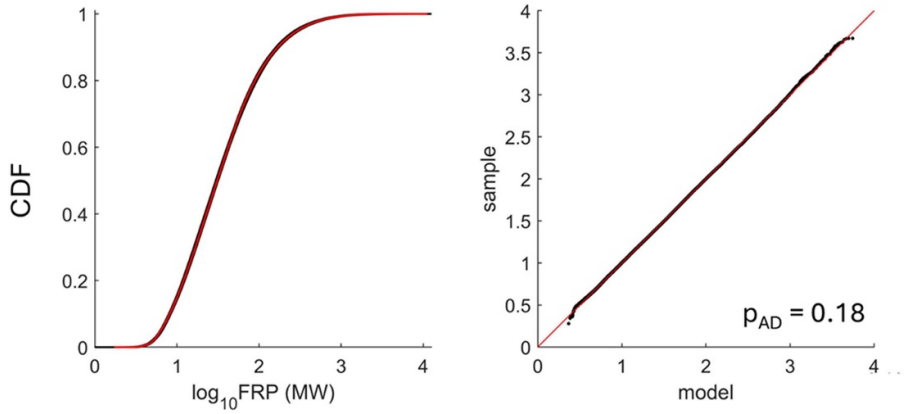

Figure 4. CDF curves of the FRP eight-parameter models (left) as obtained with maximum likelihood estimates from the entire dataset (red curve) and from the100 subsamples of 1000 randomly selected events from the dataset and *Q*–*Q* plots (right) of empirical quantiles versus model quantiles for the model fitted to the entire dataset.

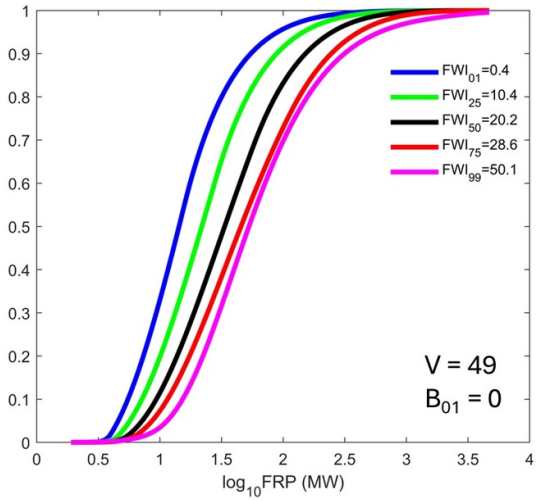

Figure 5. Distribution of log10(FRP) for percentiles 1, 25, 50, 75 and 99 of FWI as obtained from the 16-parameter model with FWI as covariate with maximum likelihood estimates for the entire dataset of FRP records and associated FWI values.

and then to RCP 8.5, an indication that the probability of occurrence of fires releasing high levels of radiative energy increases from the high-mitigation scenario to the worst-case scenario.

Differences among CDF curves are enhanced when the analysis is performed in relative terms. This is achieved by computing the exceeding ratio curve for each scenario, i.e. the ratio between the probability of exceedance curve of log10(FRP) for the scenario and that for the historical period. Results for the three scenarios are shown in figures 7(a)–(c), and the remarkable increase in exceeding ratio for larger values of log10(FRP) is worth noting. During the first projection period (2011–2030), all three scenarios show similar results. Even for the strong mitigation scenario (RCP 2.6), there is a projected increase in very intense wildfire events. For instance, in this scenario, events with log10(FRP) = 3.5 (equivalent to 3000 MW) are projected to be twice more frequent than in the historical period.

When progressing into the middle and end of the century, exceedance ratio values continue to show an upward trend. In the case of the scenario with no mitigation (RCP 8.5), extreme events with log10(FRP) = 3.5 may occur 2.5 times more frequently during the middle of the century and up to 3.5 times more frequently by the end of the century compared to the historical period. This indicates a substantial increase in the occurrence of extremely intense wildfires as we progress into the future under the RCP 8.5 scenario.

For the RCP 4.5 scenario, exceedance ratio values also show a gradual projected increase over the course of the century. Specifically, extreme events with log10(FRP) = 3 (equivalent to 1000 MW) may occur almost 1.5 times more frequently during the middle and end of the century compared to the historical period.

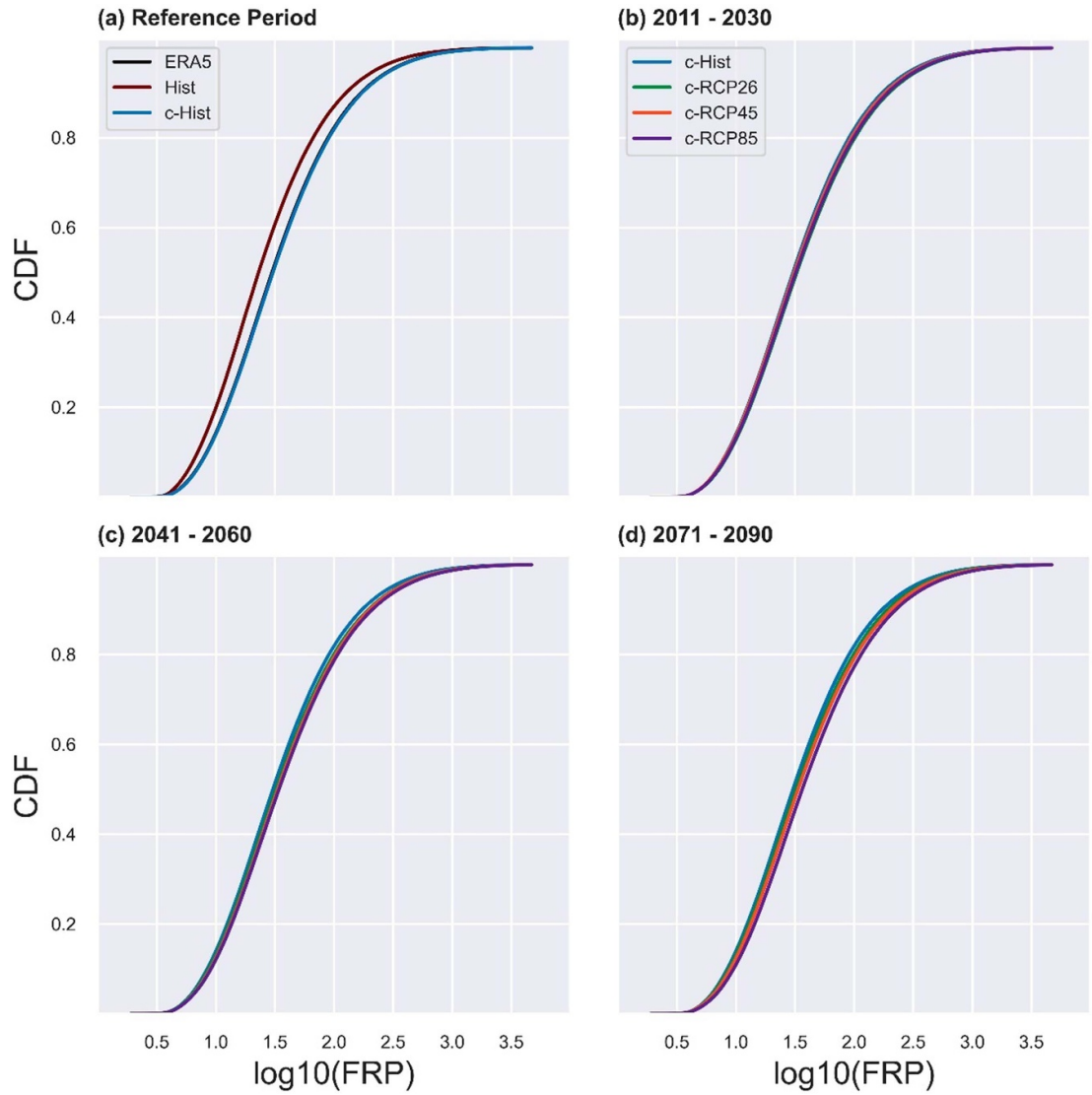

Figure 6. Distribution of synthetic log10(FRP) on vegetation fire hotspots as CDF (a) from ERA5 (solid black line), multi-model ensemble for the historical period (HIST; solid dark red line), and the bias corrected multi-model ensemble for the historical period (c-HIST; solid blue line). CDFs of bias corrected multi-model ensemble log10(FRP) for historical and projected scenarios RCP 2.6 (green line), RCP 4.5 (orange line), and RCP 8.5 (purple line) for the three 20-year future periods 2011–2030 (b), 2041–2060 (c), and 2071–2090 (d).

Although this scenario represents a moderate mitigation effort, the results still reveal a rise in the frequency of severe wildfires as the century unfolds.

When implementing the three ignition avoidance strategies, as defined in section 3.4, distinct impacts on the reduction of wildfires are observed, as depicted in figure 8. In the case of the historical simulations, Strategy 1 (figure 8 top panels) leads to a reduction in the probability of exceedance of log10(FRP) by about 10% for fires with 100 MW, about 25% for fires with 1000 MW, and up to about 40% for very intense fires. In the case of Strategy 2 (figure 8 middle panels), the projected decrease is about 15% for 100 MW, 40% for 1000 MW, and about 65% for very large log10(FRP). Finally, for Strategy 3 (figure 8 bottom panels), the impact is close to 0% for 100 MW, 20% for 1000 MW, and 45% for very large log10(FRP).

Regarding the future projections, the results for each strategy generally show larger impacts than those obtained for the historical simulation. Concerning the impact of Strategy 1, a similar behavior is observed among scenarios and time periods. For example, for 1000 MW, the impact is about 25%–30% regardless of the mitigation scenario and the time period. The impact of Strategy 2 is more dependent on the scenario and the time period. During the beginning of the century, the scenarios' curves overlap with that of the historical period. However, for the middle and end of the century, the impact becomes more pronounced, especially for RCP 8.5, with a larger reduction of wildfires compared to the historical period. For instance, at 100 MW, the impact rises from 15% to more than 20%, at 1000 MW, it increases from 40% to 50%, and for very large values of log10(FRP), it escalates from 65% to more than 75%.

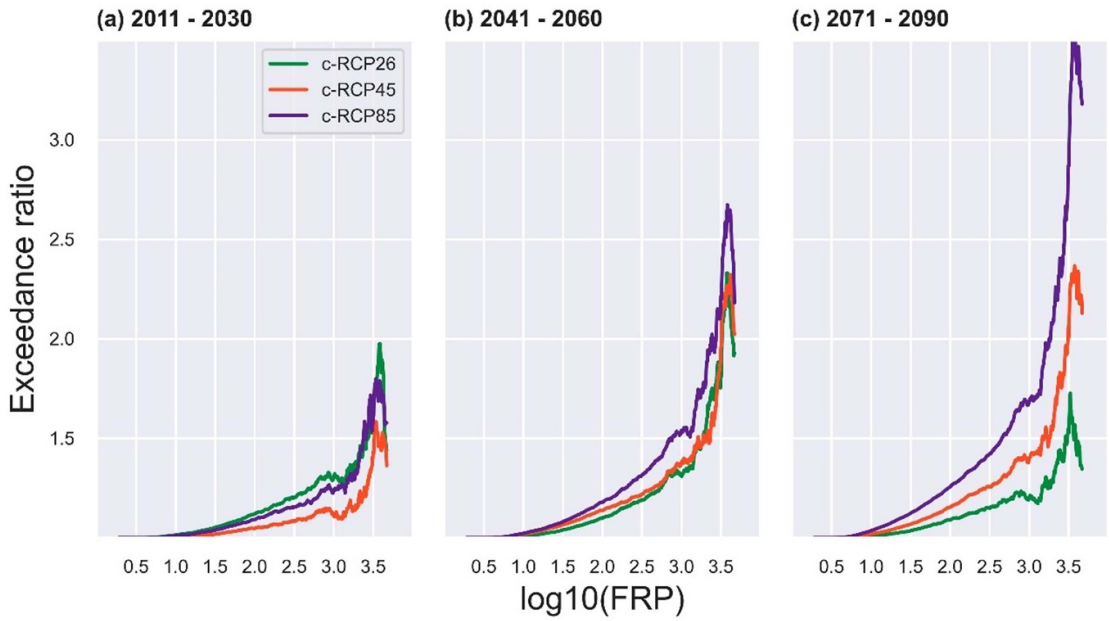

Figure 7. Exceedance ratio of log10(FRP) projected scenarios RCP 2.6 (green line), RCP 4.5 (orange line), and RCP 8.5 (purple line) relative to the historical period for the three 20-year future periods 2011–2030 (a), 2041–2060 (b), and 2071–2090 (c).

Finally, the impact of Strategy 3 reveals to be the most sensitive to mitigation scenarios and time periods. As for Strategies 1 and 2, during the beginning of the century, there are very small differences between scenarios and historical simulation. However, for RCP 8.5 in the middle and end of the century, as well as for RCP 2.6 in the middle and RCP 4.5 at the end of the century, there is a strong impact in the reduction of wildfires, reaching more than 60% for RCP 8.5 by the end of the century for very high values of log10(FRP) (compared to below 50% in the historical period).

5. Discussion

FWI is the most widely used fire danger index, and several studies have relied on FWI to assess the impact of climate change on meteorological fire danger over different regions (Abatzoglou *et al* 2019, Bento *et al* 2023; Calheiros *et al* 2021, Dupuy *et al* 2020, Fargeon *et al* 2020, Jones *et al* 2022, Varela *et al* 2019). Some of these studies focused on Portugal (Nunes *et al* 2019), and others extended their scope to encompass the Iberian Peninsula (Calheiros *et al* 2021, Santos *et al* 2023) or the western Mediterranean basin (Gouveia *et al* 2016, Pinto *et al* 2018, Varela *et al* 2019). All these studies consistently point to the fact that meteorological fire danger, mainly driven by air temperature, humidity, wind speed, and precipitation, is expected to increase under climate change in western Mediterranean, due to higher temperatures (including more summer heatwaves) and less precipitation in spring and summer (Trigo *et al* 2016, Ruffault *et al* 2020).

It is worth pointing out that meteorological fire danger is not the only driver of wildfire activity, and that other factors have to be considered, namely those related to fuel control and socioeconomic activities; for instance, Jones *et al* (2022) have shown that burned area is decreasing in Mediterranean Europe, despite the increase in FWI. However, as suggested by the results of the model of FRP, the occurrence of high intense fires (i.e. fires releasing high amounts of energy) is strongly conditioned by large values of FWI.

In line with previous studies, results of this work highlight the expected increase in probability of exceedance of FWI for three different GHG mitigation scenarios. The projected increase is particularly pronounced towards the end of the century under RCP 8.5, the most extreme scenario. These results are consistent with the projected decrease in mean precipitation, coupled with an increase in extreme precipitation events (Soares *et al* 2017, Lima *et al* 2023a) together with a substantial rise in maximum and minimum temperatures throughout all seasons and emission scenarios (Cardoso *et al* 2019, 2023) and increased 10 m wind speeds over central Portugal during summer (Nogueira *et al* 2019). The combination of higher temperatures with reduced mean precipitation and increased wind speeds in fire-prone forested areas and shrublands like those in northern and central Portugal (figure 1(b)) sets up the perfect scenario for larger, more energetic, and ultimately more destructive wildfires.

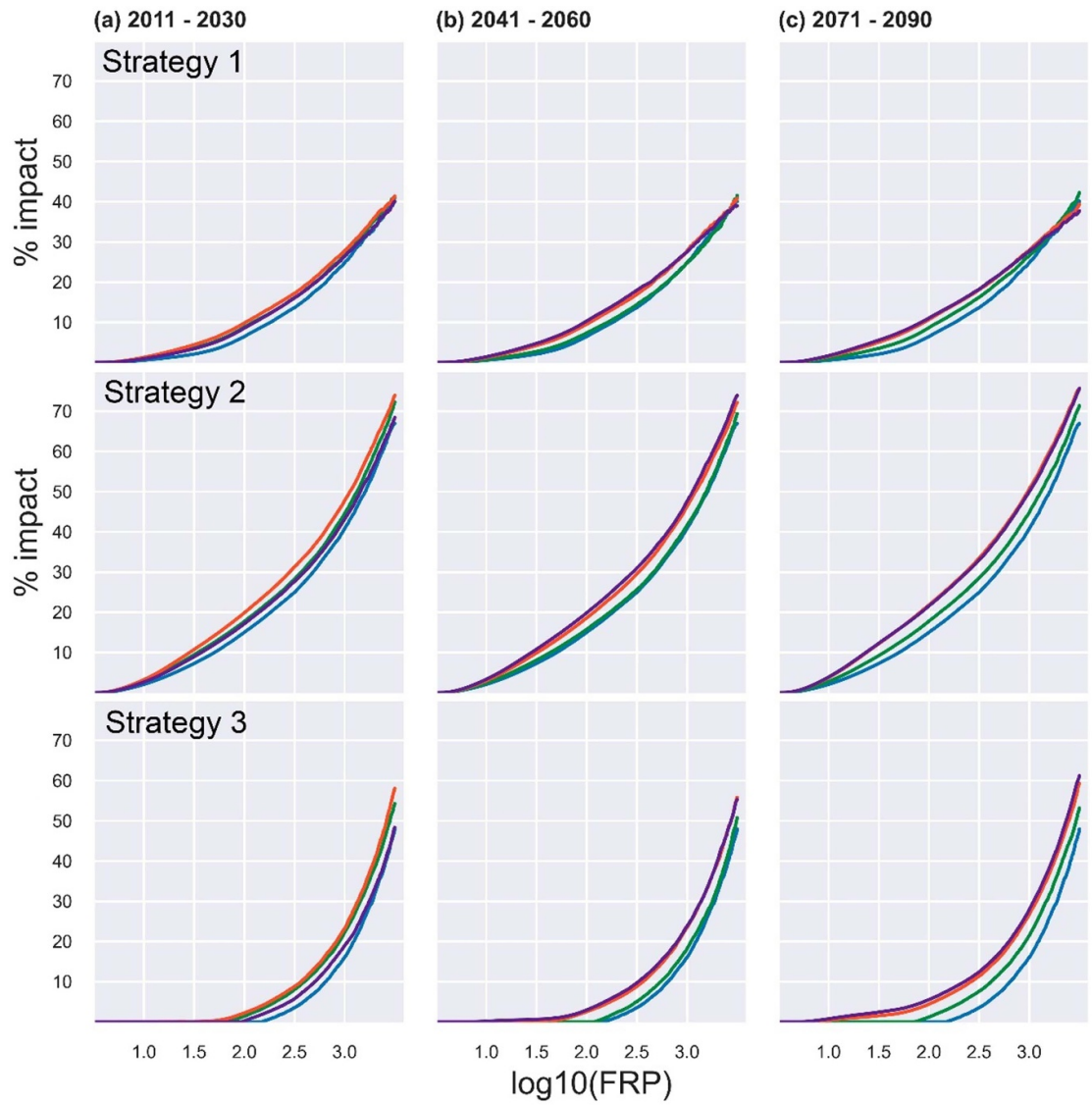

Figure 8. Impact on log10(FRP) on vegetation fire hotspots for three different adaptation strategies. Results for the historical period (blue line) and the projected scenarios RCP 2.6 (green line), RCP 4.5 (orange line), and RCP 8.5 (red line) for the three 20-year future periods 2011–2030 (a), 2041–2060 (b), and 2071–2090 (c).

This is confirmed by generating synthetic values of log10(FRP) for sets of FWI derived from projections for different climate scenarios using a statistical model with FWI as a covariate of its parameters (DaCamara *et al* 2023, Nunes *et al* 2023).

By comparing the distributions of generated values of log10(FRP) for different greenhouse gas scenarios with that generated from historical FWI, we identified a consistent increase in the probability of higher values of log10(FRP) across all RCPs and future time periods. This change is particularly pronounced under the RCP 8.5 and for more energetic wildfires, with the likelihood of experiencing a fire with energy exceeding 1000 MW in the most extreme scenario being amplified by a factor of about 1.5 and between 1.5 and 3.5 for megafires with energy exceeding 3000 MW.

Under RCP 2.6, the probability of occurrence of megafires with energy exceeding 3000 MW is expected to double by the mid-21st century yet reducing afterwards. This reduction in the later period under RCP 2.6 relates to the declining radiative forcing after under this scenario (IPCC 2023b, Soares *et al* 2023b).

The combined natural and anthropogenic-driven radiative forcings changes under RCP 4.5 and RCP 8.5 are distinctly reflected in our results. Indeed, RCP 4.5 shows a gradual increase in forcing until 2060, followed by stabilization, leading to similar values of probability exceedances of log10(FRP) for mid- and end-century. In contrast, RCP 8.5 exhibits a relentless increase in radiative forcing that leads to a continuous increase in the probability of exceedance across all future time periods.

These findings call for urgent and effective fire prevention strategies aiming to attenuate the potential impact of climate change on wildfire occurrences. Even with ambitious efforts to reduce emissions (RCP

2.6), the risk of encountering highly energetic wildfires remains a significant concern. The continuous increase in FRP probabilities under more severe emission scenarios (RCP 4.5 and RCP 8.5) highlights the pressing need for comprehensive and adaptive wildfire management strategies to safeguard communities and ecosystems in the face of escalating fire risks.

We considered three ignition avoidance strategies and analyzed their impacts on probability of occurrence of high intensity fires, i.e. of fires releasing high amounts of energy:

Strategy 1, involving a random reduction of 50% of FRPs when FWI exceeds the sample median, showcased appreciable reductions in the probability of exceedance of log10(FRP) across all energy thresholds. Notably, fires with an energy release of 100 MW showed a decrease of about 10%, whereas those with 1000 MW and very high log10(FRP) revealed reductions of about 25% and 40%, respectively. This strategy showed to be promising to curb fire occurrences in moderate fire weather conditions, however it does not deal very effectively with the most intense fires.

In the case of Strategy 2, where 50%, 90%, and 95% of log10(FRP) were randomly reduced for FWI ranging between the 75th and 90th sample percentiles, 90th and 95th sample percentiles, and above 95th sample percentile, respectively, the impact was more pronounced than in Strategy 1. The probability of exceedance decreased by approximately 15%, 40%, and 70% for 100 MW, 1000 MW, and very large FRP, respectively.

Finally, Strategy 3 involved the random reduction of 95% of FRPs when FWI exceeded the 95th sample percentile. Although showing smaller reductions when compared to Strategy 2, with decreases of around 0%, 20% and 50% for 100 MW, 1000 MW, and maximum FRP, Strategy 3 proved effective in reducing the occurrence of extremely intense fires during the most critical fire weather conditions and may lead to less but more focused resources.

It may be noted that the impacts of strategy 2 are higher than those of the other two, both for historical and future scenarios. Although with less impact than Strategy 2, Strategy 3 represents a compromises between Strategies 1 and 2, and specifically addresses the increasing challenges posed by extreme fire weather events under climate change scenarios.

We acknowledge that this study is not without its limitations, and some caveats need to be considered when interpreting the results. The first limitation pertains to the assumption of static vegetation in the future projections. By assuming that the same areas that experienced wildfires during the historical period of 2001–2020 will remain unchanged in the future, we overlook the potential impact of climate change on vegetation structure (Seidl *et al* 2017, Bento *et al* 2021, Nolan *et al* 2021). Adaptation strategies to climate change may involve altering the landscape's vegetation (Chausson *et al* 2020), and as aridity increases in the region (Andrade *et al* 2021), the types of vegetation might naturally shift. To address this limitation, ongoing efforts are exploring the use of new vegetation maps that evolve over time based on the shared socioeconomic pathway scenarios.

Another potential limitation lies in the lack of interpretation of the three ignition avoidance strategies, particularly regarding the operational ways to implement them, as well as the costs and human and material effort involved. One has however to consider that the intent of this work was to assess the impact of ignition avoidance on the probability of occurrence of high intensity vegetation fires, and ultimately to point out the benefits of adopting strategies that take into account the temporal and spatial distribution of meteorological fire danger.

6. Final remarks

This study has shed light on the concerning trend of very energetic fires in continental Portugal, where the probability of occurrence may increase by 1.5 to more than three-fold, depending on the mitigation pathway pursued. Even if high mitigation scenarios are successfully achieved, the probability of experiencing megafires is still expected to increase by a factor of almost 2.5 in the middle of the century. These results underscore the need for adaptation measures, irrespective of the chosen mitigation strategy. While ad-hoc strategies might prove effective for small to medium-sized fires, addressing the challenge of very large fires requires concrete and well-prepared strategies, both from a political and societal perspective. A paradigm shift, centered on caution and preservation, is crucial for navigating these increasing fire risks.

This study also highlights the pressing importance of taking timely and proactive action to combat the escalating risk of wildfires fueled by climate change. It calls for a comprehensive approach that combines mitigation efforts with well-prepared adaptation strategies. By adopting a forward-thinking mindset, emphasizing caution and preservation, society can collectively rise to the challenge of minimizing the impact of wildfires in the face of a changing climate. Policymakers, communities, and stakeholders must work in unison to develop effective and efficient measures that safeguard lives, ecosystems, and economies in the

years to come. Only through collaborative efforts and a commitment to prioritizing the preservation of our environment can we secure a more resilient and sustainable future.

Data availability statement

All data that support the findings of this study are included within the article (and any supplementary information files).

Acknowledgments

The authors acknowledge the EEA-Financial Mechanism 2014- 2021 and the Portuguese Environment Agency through Pre-defined Project-2 National Roadmap for Adaptation XXI (PDP-2) and the DHEFEUS project (2022.09185.PTDC) funded by FCT. The authors would also like to acknowledge the project 'CEASEFIRE: Envio e disseminação de alertas automatizados de gestão de perigo meteorológico de incêndio', financed by The Navigator Company.

Author contributions

Carlos C DaCamara: Conceptualization, Methodology, Formal Analysis, Writing—Review & Editing. Virgílio A Bento: Conceptualization, Methodology, Validation, Formal Analysis, Writing—Original Draft, Visualization. Silvía A Nunes: Resources, Data Curation. Gil Lemos: Resources, Software. Pedro M M Soares: Validation, Writing—Review & Editing. Ricardo M Trigo: Conceptualization, Writing—Review & Editing.

Conflict of interest

The authors declare that they have no conflict of interest.

Financial Support

This work was funded by the Portuguese Fundação para a Ciência e a Tecnologia (FCT) I.P./MCTES through national funds (PIDDAC) – UIDB/50019/2020 (https://doi.org/10.54499/UIDB/50019/2020), UIDP/50019/2020 (https://doi.org/10.54499/UIDP/50019/2020) and LA/P/0068/2020 (https://doi.org/10.54499/LA/P/0068/2020). This work was performed under the scope of project https://doi.org/10.54499/2022.09185.PTDC (DHEFEUS) and supported by national funds through FCT. The authors would like to acknowledge the project 'CEASEFIRE: Envio e disseminação de alertas automatizados de gestão de perigo meteorológico de incêndio', financed by The Navigator Company.

ORCID iDs

Virgílio A Bento https://orcid.org/0000-0001-9574-3090
Gil Lemos https://orcid.org/0000-0002-2585-6871

References

Abatzoglou J T, Williams A P and Barbero R 2019 Global emergence of anthropogenic climate change in fire weather indices *Geophys. Res. Lett.* **46** 326–36

Amraoui M, Liberato M L R, Calado T J, DaCamara C C, Coelho L P, Trigo R M and Gouveia C M 2013 Fire activity over Mediterranean Europe based on information from Meteosat-8 *For. Ecol. Manage.* **294** 62–75

Andrade C, Contente J and Santos J A 2021 Climate change projections of aridity conditions in the iberian Peninsula *Water* **13** 2035

Austin K G, Baker J S, Sohngen B L, Wade C M, Daigneault A, Ohrel S B, Ragnauth S and Bean A 2020 The economic costs of planting, preserving, and managing the world's forests to mitigate climate change *Nat. Commun.* **11** 1–9

Bento V A, Ribeiro A F S, Russo A, Gouveia C M, Cardoso R M and Soares P M M 2021 The impact of climate change in wheat and barley yields in the Iberian Peninsula *Sci. Rep.* **11** 1–12

Bento V A, Russo A, Gouveia C M and Dacamara C C 2022 Recent change of burned area associated with summer heat extremes over Iberia *Int. J. Wildland Fire* **31** 658–69

Bento V A, Russo A, Vieira I and Gouveia C M 2023 Identification of forest vulnerability to droughts in the Iberian Peninsula *Theor. Appl. Climatol.* **152** 559–79

Boer M M, Resco de Dios V and Bradstock R A 2020 Unprecedented burn area of Australian mega forest fires *Nat. Clim. Change* **10** 171–2

Brunner L, Lorenz R, Zumwald M and Knutti R 2019 Quantifying uncertainty in European climate projections using combined performance-independence weighting *Environ. Res. Lett.* **14** 124010

Buchhorn M, Lesiv M, Tsendbazar N E, Herold M, Bertels L and Smets B 2020 Copernicus global land cover layers—collection 2 *Remote Sens.***12** 1044

Calheiros T, Pereira M G and Nunes J P 2021 Assessing impacts of future climate change on extreme fire weather and pyro-regions in Iberian Peninsula *Sci. Total Environ.* **754** 142233
Cardoso R M, Lima D C A and Soares P M M 2023 How persistent and hazardous will extreme temperature events become in a warming Portugal? *Weather Clim. Extrem.* **41** 100600
Cardoso R M and Soares P M M 2022 Is there added value in the EURO-CORDEX hindcast temperature simulations? Assessing the added value using climate distributions in Europe *Int. J. Climatol.* **42** 4024–39
Cardoso R M, Soares P M M, Lima D C A and Miranda P M A 2019 Mean and extreme temperatures in a warming climate: EURO CORDEX and WRF regional climate high-resolution projections for Portugal *Clim. Dyn.* **52** 129–57
Careto J A, Soares P M, Cardoso R M, Herrera S and Gutiérrez J M 2022a Added value of EURO-CORDEX high-resolution downscaling over the Iberian Peninsula revisited—Part 1: Precipitation *Geosci. Model Dev.* **15** 2635–52
Careto J A, Soares P M, Cardoso R M, Herrera S and Gutiérrez J M 2022b Added value of EURO-CORDEX high-resolution downscaling over the Iberian Peninsula revisited—Part 2: Max and min temperature *Geosci. Model Dev.* **15** 2653–71
Carrillo J, Pérez J C, Expósito F J, Díaz J P and González A 2022 Projections of wildfire weather danger in the Canary Islands *Sci. Rep.* **12** 1–12
Carvalho A, Flannigan M D, Logan K A, Gowman L M, Miranda A I and Borrego C 2009 The impact of spatial resolution on area burned and fire occurrence projections in Portugal under climate change *Clim. Change* **98** 177–97
Chausson A *et al* 2020 Mapping the effectiveness of nature-based solutions for climate change adaptation *Glob. Change Biol.* **26** 6134–55
DaCamara C C, Calado T J, Ermida S L, Trigo I F, Amraoui M and Turkman K F 2014 Calibration of the fire weather index over mediterranean Europe based on fire activity retrieved from MSG satellite imagery *Int. J. Wildland Fire* **23** 945–58
DaCamara C C, Libonati R, Nunes S A, de Zea Bermudez P and Pereira J M C 2023 Global-scale statistical modelling of the radiative power released by vegetation fires using a doubly truncated lognormal body distribution with generalized Pareto tails *Physica A* **625** 129049
DGAPPF/DDFVAP 2018 6° Relatório provisório de incêndios rurais—2018
Diffenbaugh N S and Giorgi F 2012 Climate change hotspots in the CMIP5 global climate model ensemble *Clim. Change* **114** 813–22
Dupuy J L, Fargeon H, Martin-StPaul N, Pimont F, Ruffault J, Guijarro M, Hernando C, Madrigal J and Fernandes P 2020 Climate change impact on future wildfire danger and activity in southern Europe: a review *Ann. For. Sci.* **77** 35
Eyring V *et al* 2019 Taking climate model evaluation to the next level *Nat. Clim. Change* **9** 102–10
Faggian P 2018 Estimating fire danger over Italy in the next decades *Euro-Mediterranean J. Environ. Integr.* **3** 1–13
Fargeon H, Pimont F, Martin-StPaul N, De Caceres M, Ruffault J, Barbero R and Dupuy J L 2020 Projections of fire danger under climate change over France: where do the greatest uncertainties lie? *Clim. Change* **160** 479–93
Garcia-Herrera R, Díaz J, Trigo R M, Luterbacher J and Fischer E M 2010 A review of the european summer heat wave of 2003 *Crit. Rev. Environ. Sci. Technol.* **40** 267–306
Giannakopoulos C, Le Sager P, Bindi M, Moriondo M, Kostopoulou E and Goodess C M 2009 Climatic changes and associated impacts in the Mediterranean resulting from a 2 °C global warming *Glob. Planet. Change* **68** 209–24
Giglio L , Schroeder W , Hall J V and Justice C O 2020 *MODIS Collection 6 and Collection 6.1 Active Fire Product User's Guide* (National Aeronautical and Space Administration—NASA) (available at: https://modis-land.gsfc.nasa.gov/pdf/MODIS_C6_C6.1_Fire_User_Guide_1.0.pdf)
Giorgi F 2006 Climate change hot-spots *Geophys. Res. Lett.* **33**
Giorgi F, Jones C and Asrar G 2009 Addressing climate information needs at the regional level: the CORDEX framework *WMO Bull.* **58** 175 (available at: https://cordex.org/wp-content/uploads/2018/03/cordex_giorgi_wmo.pdf)
Gouveia C M, Bistinas I, Liberato M L R, Bastos A, Koutsias N and Trigo R 2016 The outstanding synergy between drought, heatwaves and fuel on the 2007 Southern Greece exceptional fire season *Agric. For. Meteorol.* **218–219** 135–45
Gumbel E 1935 Les valeurs extrêmes des distributions statistiques *Ann. l'institut Henri Poincaré* **2** 115–58
Gutiérrez J M *et al* 2019 An intercomparison of a large ensemble of statistical downscaling methods over Europe: results from the VALUE perfect predictor cross-validation experiment *Int. J. Climatol.* **39** 3750–85
Haerter J O, Hagemann S, Moseley C and Piani C 2011 Climate model bias correction and the role of timescales *Hydrol. Earth Syst. Sci.* **15** 1065–79
Herrera S, Bedia J, Gutiérrez J M, Fernández J and Moreno J M 2013 On the projection of future fire danger conditions with various instantaneous/mean-daily data sources *Clim. Change* **118** 827–40
Herrera S, Soares P M M, Cardoso R M and Gutiérrez J M 2020 Evaluation of the EURO-CORDEX regional climate models over the Iberian Peninsula: observational uncertainty analysis *J. Geophys. Res. Atmos.* **125** e2020JD032880
Hersbach H *et al* 2020 The ERA5 global reanalysis *Q. J. R. Meteorol. Soc.* **146** 1999–2049
Hertig E, Maraun D, Bartholy J, Pongracz R, Vrac M, Mares I, Gutiérrez J M, Wibig J, Casanueva A and Soares P M M 2019 Comparison of statistical downscaling methods with respect to extreme events over Europe: validation results from the perfect predictor experiment of the COST Action VALUE *Int. J. Climatol.* **39** 3846–67
IPCC 2023a *Climate Change 2022: Impacts, Adaptation and Vulnerability*
IPCC 2023b *Climate Change 2021—The Physical Science Basis, Climate Change 2021—The Physical Science Basis* (https://doi.org/10.1017/9781009157896)
Jacob D *et al* 2014 EURO-CORDEX: new high-resolution climate change projections for European impact research *Reg. Environ. Change* **14** 563–78
Jacob D *et al* 2020 Regional climate downscaling over Europe: perspectives from the EURO-CORDEX community *Reg. Environ. Change* **20** 1–20
Jones M W *et al* 2022 Global and regional trends and drivers of fire under climate change *Rev. Geophys.* **60** e2020RG000726
Katragkou E *et al* 2015 Regional climate hindcast simulations within EURO-CORDEX: evaluation of a WRF multi-physics ensemble *Geosci. Model. Dev.* **8** 603–61
Keeley J E and Syphard A D 2019 Twenty-first century California, USA, wildfires: fuel-dominated vs. wind-dominated fires *Fire Ecol.* **15** 1–15
Kotlarski S *et al* 2014 Regional climate modeling on European scales: a joint standard evaluation of the EURO-CORDEX RCM ensemble *Geosci. Model. Dev.* **7** 1297–333
Krawchuk M A, Moritz M A, Parisien M A, Van Dorn J and Hayhoe K 2009 Global pyrogeography: the current and future distribution of wildfire *PLoS One* **4** e5102
Lemos G, Menendez M, Semedo A, Camus P, Hemer M, Dobrynin M and Miranda P M A 2020a On the need of bias correction methods for wave climate projections *Glob. Planet. Change* **186** 103109

Lemos G, Semedo A, Dobrynin M, Menendez M and Miranda P M A 2020b Bias-corrected cmip5-derived single-forcing future wind-wave climate projections toward the end of the twenty-first century *J. Appl. Meteorol. Climatol.* **59** 1393–414
Libonati R *et al* 2021 Twenty-first century droughts have not increasingly exacerbated fire season severity in the Brazilian Amazon *Sci. Rep.* **11** 1–13
Libonati R *et al* 2022 Assessing the role of compound drought and heatwave events on unprecedented 2020 wildfires in the Pantanal *Environ. Res. Lett.* **17** 015005
Lima D C A, Bento V A, Lemos G, Nogueira M and Soares P M M 2023a A multi-variable constrained ensemble of regional climate projections under multi-scenarios for Portugal—part II: sectoral climate indices *Clim. Serv.* **30** 100377
Lima D C A, Lemos G, Bento V A, Nogueira M and Soares P M M 2023b A multi-variable constrained ensemble of regional climate projections under multi-scenarios for Portugal—part I: an overview of impacts on means and extremes *Clim. Serv.* **30** 100351
Maraun D *et al* 2017 Towards process-informed bias correction of climate change simulations *Nat. Clim. Change* **7** 764–73
Maraun D *et al* 2019 The VALUE perfect predictor experiment: evaluation of temporal variability *Int. J. Climatol.* **39** 3786–818
Marin M, Clinciu I, Tudose N C, Ungurean C, Adorjani A, Mihalache A L, Davidescu A A, Davidescu Şerban O, Dinca L and Cacovean H 2020 Assessing the vulnerability of water resources in the context of climate changes in a small forested watershed using SWAT: a review *Environ. Res.* **184** 109330
Mendonça J M and Máguas C 2023 Relatório Final do Grupo de Peritos dos Incêndios Rurais
Moemken J, Reyers M, Feldmann H and Pinto J G 2018 Future changes of wind speed and wind energy potentials in EURO-CORDEX ensemble simulations *JGR Atmos.* **123** 6373–89
Molina M O, Careto J A M, Gutiérrez C, Sánchez E and Soares P M M 2023 The added value of high-resolution EURO-CORDEX simulations to describe daily wind speed over Europe *Int. J. Climatol.* **43** 1062–78
Moriondo M, Good P, Durao R, Bindi M, Giannakopoulos C and Corte-Real J 2006 Potential impact of climate change on fire risk in the Mediterranean area *Clim. Res.* **31** 85–95
Nogueira M, Soares P M M, Tomé R and Cardoso R M 2019 High-resolution multi-model projections of onshore wind resources over Portugal under a changing climate *Theor. Appl. Climatol.* **136** 347–62
Nolan R H, Collins L, Leigh A, Ooi M K J, Curran T J, Fairman T A, Resco de Dios V and Bradstock R 2021 Limits to post-fire vegetation recovery under climate change *Plant Cell Environ.* **44** 3471–89
Nunes S A, DaCamara C C, Pereira J M C and Trigo R M 2023 Assessing the role played by meteorological conditions on the interannual variability of fire activity in four subregions of Iberia *Int. J. Wildland Fire* **32** 1529–41
Nunes S A, Dacamara C C, Turkman K F, Calado T J, Trigo R M and Turkman M A A 2019 Wildland fire potential outlooks for Portugal using meteorological indices of fire danger *Nat. Hazards Earth Syst. Sci.* **19** 1459–70
Pausas J G and Keeley J E 2021 Wildfires and global change *Front. Ecol. Environ.* **19** 387–95
Pausas J G, Llovet J, Rodrigo A and Vallejo R 2008 Are wildfires a disaster in the Mediterranean basin? – A review *Int. J. Wildland Fire* **17** 713–23
Pereira M G, Trigo R M, da Camara C C, Pereira J M C and Leite S M 2005 Synoptic patterns associated with large summer forest fires in Portugal *Agr. Forest Metrol.* **129** 11–25
Pinto M M, DaCamara C C, Trigo I F, Trigo R M and Turkman K F 2018 Fire danger rating over Mediterranean Europe based on fire radiative power derived from Meteosat *Nat. Hazards Earth Syst. Sci.* **18** 515–29
Prein A F *et al* 2016 Precipitation in the EURO-CORDEX 0.11 and 0.44 simulations: high resolution, high benefits? *Clim. Dyn.* **46** 383–412
Ramos A M, Russo A, DaCamara C C, Nunes S, Sousa P, Soares P M M, Lima M M, Hurduc A and Trigo R M 2023 The compound event that triggered the destructive fires of October 2017 in Portugal *iScience* **26** 106141
Rocheta E, Evans J P and Sharma A 2017 Can bias correction of regional climate model lateral boundary conditions improve low-frequency rainfall variability? *J. Clim.* **30** 9785–806
Romanello M *et al* 2022 The 2022 report of the lancet countdown on health and climate change: health at the mercy of fossil fuels *Lancet* **400** 1619–54
Ruffault J *et al* 2020 Increased likelihood of heat-induced large wildfires in the Mediterranean Basin *Sci. Rep.* **10** 1–9
Ruffault J, Curt T, Martin-Stpaul N K, Moron V and Trigo R M 2018 Extreme wildfire events are linked to global-change-type droughts in the northern Mediterranean *Nat. Hazards Earth Syst. Sci.* **18** 847–56
Rummukainen M 2010 State-of-the-art with regional climate models. Wiley Interdiscip *Rev. Clim. Change* **1** 82–96
Russo A, Gouveia C M, Páscoa P, DaCamara C C, Sousa P M and Trigo R M 2017 Assessing the role of drought events on wildfires in the Iberian Peninsula *Agric. For. Meteorol.* **237–238** 50–59
San-Miguel-Ayanz J *et al* 2012 Comprehensive monitoring of wildfires in Europe: the European forest fire information system (EFFIS) *Approaches to Managing Disaster—Assessing Hazards, Emergencies and Disaster Impacts* (IntechOpen) (https://doi.org/10.5772/28441)
San-Miguel-Ayanz J *et al* (Joint Research Centre—European Commission) 2023 *Advance Report on Forest Fires in Europe, Middle East and North Africa 2022* (Publications Office of the European Union) (https://doi.org/10.2760/091540)
Sánchez-Benítez A, García-Herrera R, Barriopedro D, Sousa P M and Trigo R M 2018 June 2017: the earliest European summer mega-heatwave of reanalysis period *Geophys. Res. Lett.* **45** 1955–62
Santos L C, Lima M M, Bento V A, Nunes S A, DaCamara C C, Russo A, Soares P M M and Trigo R M 2023 An evaluation of the atmospheric instability effect on wildfire danger using ERA5 over the Iberian Peninsula *Fire* **6** 120
Seidl R *et al* 2017 Forest disturbances under climate change *Nat. Clim. Change* **7** 395–402
Shahzad A, Ullah S, Dar A A, Sardar M F, Mehmood T, Tufail M A, Shakoor A and Haris M 2021 Nexus on climate change: agriculture and possible solution to cope future climate change stresses *Environ. Sci. Pollut. Res.* **28** 14211–32
Soares P M M *et al* 2019 Process-based evaluation of the VALUE perfect predictor experiment of statistical downscaling methods *Int. J. Climatol.* **39** 3868–93
Soares P M M, Cardoso R M, Lima D C A and Miranda P M A 2017 Future precipitation in Portugal: high-resolution projections using WRF model and EURO-CORDEX multi-model ensembles *Clim. Dyn.* **49** 2503–30
Soares P M M, Cardoso R M, Miranda P M A, Viterbo P and Belo-Pereira M 2012 Assessment of the ENSEMBLES regional climate models in the representation of precipitation variability and extremes over Portugal *J. Geophys. Res. Atmos.* **117** 7114
Soares P M M, Careto J A M, Russo A and Lima D C A 2023a The future of Iberian droughts: a deeper analysis based on multi-scenario and a multi-model ensemble approach *Nat. Hazards* **117** 2001–28
Soares P M M, Lemos G and Lima D C A 2023b Critical analysis of CMIPs past climate model projections in a regional context: the Iberian climate *Int. J. Climatol.* **43** 2250–70

Soares P M M and Lima D C A 2022 Water scarcity down to earth surface in a Mediterranean climate: the extreme future of soil moisture in Portugal *J. Hydrol.* **615** 128731
Soares P M and Cardoso R M 2018 A simple method to assess the added value using high-resolution climate distributions: application to the EURO-CORDEX daily precipitation *Int. J. Climatol.* **38** 1484–98
Stocks B J, Lynham T J, Lawson B D, Alexander M E, Wagner C E V, McAlpine R S and Dubé D E 1989 The Canadian forest fire danger rating system: an overview *For. Chron.* **65** 450–7
Trigo I F *et al* 2011 The satellite application facility for land surface analysis *Int. J. Remote Sens.* **32** 2725–44
Trigo R M, Pereira J M C, Pereira M G, Mota B, Calado T J, Dacamara C C and Santo F E 2006 Atmospheric conditions associated with the exceptional fire season of 2003 in Portugal *Int. J. Climatol.* **26** 1741–57
Trigo R M, Sousa P M, Pereira M G, Rasilla D and Gouveia C M 2016 Modelling wildfire activity in Iberia with different atmospheric circulation weather types *Int. J. Climatol.* **36** 2761–78
Trnka M *et al* 2021 Observed and estimated consequences of climate change for the fire weather regime in the moist-temperate climate of the Czech Republic *Agric. For. Meteorol.* **310** 108583
Turco M, Jerez S, Augusto S, Tarín-Carrasco P, Ratola N, Jiménez-Guerrero P and Trigo R M 2019 Climate drivers of the 2017 devastating fires in Portugal *Sci. Rep.* **9** 1–8
van der Laan E, Nunes J P, Dias L F, Carvalho S and Santos F 2023 Climate change adaptability of sustainable land management practices regarding water availability and quality: a case study in the Sorraia catchment, Portugal *Sci. Total Environ.* **897** 165438
Van Wagner C E 1974 A spread index for crown fires in spring *Inf Rep*
Van Wagner C E 1987 *Development and structure of the canadian forest fire weather index system* (Canadian Forest Service)
Varela V, Vlachogiannis D, Sfetsos A, Karozis S, Politi N and Giroud F 2019 Projection of forest fire danger due to climate change in the French Mediterranean region *Sustainability* **11** 4284
Vautard R *et al* 2013 The simulation of European heat waves from an ensemble of regional climate models within the EURO-CORDEX project *Clim. Dyn.* **41** 2555–75
Vitolo C, Di Giuseppe F, Barnard C, Coughlan R, San-Miguel-Ayanz J, Libertá G and Krzeminski B 2020 ERA5-based global meteorological wildfire danger maps *Sci. Data* **7** 1–11
Wilks D S 2011 *Statistical Methods in the Atmospheric Sciences* (Academic)
World Health Organization 2021 *COP26 Special Report on Climate Change and Health: The Health Argument for Climate Action*